Aerosol and Air Quality Research, 16: 977–989, 2016

ISSN: 1680-8584 print / 2071-1409 online
doi: 10.4209/aaqr.2015.01.0057

Satellite and Ground Observations of Severe Air Pollution Episodes in the Winter of 2013 in Beijing, China

Shenshen Li[1], Zongwei Ma[2], Xiaozhen Xiong[3], David C. Christiani[4], Zhaoxi Wang[4], Yang Liu[2*]**

[1] State Key Laboratory of Remote Sensing Science, Institute of Remote Sensing and Digital Earth, Chinese Academy of Sciences. Beijing, 100101, China
[2] Emory University, Rollins School of Public Health, 1518 Clifton Road NE, Atlanta, GA 30322, USA
[3] NOAA Center for Satellite Applications and Research, 5830 University Research Ct, College Park, MD 20740, USA
[4] Harvard T.H. Chan School of Public Health, 655 Huntington Avenue, Boston, MA 02115, USA

ABSTRACT

Beginning in early January 2013, Beijing experienced multiple prolonged and severe smog events that were characterized by very high levels of $PM_{2.5}$, with peak daily $PM_{2.5}$ over 400 μg m^{-3}. With $PM_{2.5}$ concentration contours created from ground observations and satellite remote sensing data, we describe the spatial and temporal characteristics of these episodes and further investigated the factors that contributed to these episodes. Our results indicated that these smog episodes affected a much larger geographic region, far beyond Beijing metropolitan area, corresponding to a total area of ~550,000 km^2 and ~180 million people. The extremely cold weather in December 2012 and regional pollution transport were likely the main causes of these severe PM pollutions. In addition to aggressive emission control measures for Beijing, coordinated regional policy must be put in place to achieve more blue-sky days. Although the configuration of the current ground monitoring network may be sufficient to record $PM_{2.5}$ levels in urban centers, these monitors alone cannot fully characterize the spatial pattern and track the transport of air pollution on a regional scale. Satellite remote sensing data can provide valuable information to fill the gaps left by ground monitors to create a more comprehensive picture of $PM_{2.5}$.

Keywords: Smog; MODIS; Aerosol optical depth; $PM_{2.5}$; HYSPLIT.

INTRODUCTION

Smog, or the mixture of smoke and fog, is a severe air pollution event often characterized by hazy air and reduced visibility. Smog episodes can be caused by various natural and anthropogenic factors, such as forest fires, agricultural burning, fossil fuel combustion, and industrial emissions; and are exacerbated by unfavorable meteorological conditions. It is a serious problem in many large cities in the world and continues to harm human health (Chen *et al.*, 2007). During the last century, there were several well-known lethal smog episodes, including the air pollution events, in the heavily industrialized Meuse Valley (Belgium) in December 1930, in Donora (the United States) in October 1948, and in London (the United Kingdom) in December 1952. These events were associated with a significant increase of emergency room visits and deaths (Nemery *et al.*, 2001; Bell *et al.*, 2004; Chen *et al.*, 2007). China has maintained rapid economic growth, with an annual GDP growth rate of over 8% for the past two decades, largely through energy-intensive construction of infrastructure such as highways, railways and cities (Zhang *et al.*, 2012). Meanwhile, environmental pollution, especially heavy haze, is starting to take its toll. Because of its small size, $PM_{2.5}$ (airborne particles less than 2.5 micrometers in aerodynamic diameter), a major pollutant during smog events, is more likely than larger particles to carry toxic heavy metals, acid oxides, organic pollutants, and other chemicals, as well as bacteria and viruses, deep into the lungs. Exposure to $PM_{2.5}$ has been linked to various adverse health outcomes, including cardiovascular and respiratory morbidity and mortality (Pope and Dockery, 2006). Exposure to ambient $PM_{2.5}$ was recently ranked the 8th leading factor of the global burden of disease, contributing 3.2 million premature deaths worldwide in 2010 (Lim *et al.*, 2012). Moreover, on October 17, 2013, the WHO International Agency for Research on Cancer (IARC) announced that it has classified outdoor air pollution and, separately, particulate matter (PM), as carcinogenic to humans (Group 1) (Loomis *et al.*, 2013).

* Corresponding author.
Tel.: 1-404-727-2131; Fax: 1-404-727-8744
E-mail address: yang.liu@emory.edu
** Corresponding author.
Tel.: 1-617-432-4026
E-mail address: mikewang@hohp.harvard.edu

The major challenge of pollution control in China is that the environmental control measures have not kept up with the growth of its economy and energy consumption, despite China's tremendous efforts to reduce air pollution, such as by requiring newly constructed coal-fired power plants to install flue-gas desulphurization systems and strengthening vehicle-emissions standards (Zhang *et al.*, 2012). Air-quality control is further hampered by the low priority given to environmental protection and the lack of cooperation among different government agencies. $PM_{2.5}$ was not regulated in China until the beginning of 2013, despite the number of studies undertaken in the previous decade to quantify and characterize $PM_{2.5}$ (Chan and Yao, 2008; Yang *et al.*, 2011). Starting from December 2012, a nation-wide $PM_{2.5}$ monitoring network was established in China. However, the spatial distribution of these $PM_{2.5}$ monitoring stations is heavily biased towards major cities in China, with very limited coverage elsewhere.

Unlike point measurements from ground monitors, satellite remote sensing provides extensive spatial coverage. Since the launch of the Terra satellite by the U.S. National Aeronautics and Space Administration (NASA) on December 18, 1999, extensive research has explored the potential of using satellite retrieved aerosol optical depth (AOD) to estimate ground level $PM_{2.5}$ concentrations (Hoff and Christopher, 2009). AOD is a dimensionless measure of particle optical abundance defined as the integral of aerosol extinction coefficients along the vertical atmospheric column from the ground to the top of the atmosphere. When most particles are generated near the surface and well mixed in the boundary layer, AOD has been shown to be a strong predictor of $PM_{2.5}$ concentrations after accounting for the changes of particle composition and size distribution (Liu *et al.*, 2005; Liu *et al.*, 2009b; Lee *et al.*, 2011; Kloog *et al.*, 2012; Hu *et al.*, 2013; Hu *et al.*, 2014). Ma *et al.* (2014) developed a geographically weighted regression (GWR) model with satellite AOD, meteorological and land use data to predict the $PM_{2.5}$ concentrations in China, which is the first study that utilized the advanced statistical model to estimate ground PM levels with AOD in China The cross-validation R^2 of daily predicted $PM_{2.5}$ concentration on a 50 km grid reached 0.64. Several studies in China revealed various correlations between the ground PM_{10} concentrations and satellite retrieved AOD (Liu *et al.*, 2009a; Song *et al.*, 2009; Qu *et al.*, 2010). Although AOD retrieved using visible and near IR bands is mostly sensitive to fine particles, these correlations could be partially explained by changes in fine particles that had high extinction efficiencies but contribute little to the PM_{10} mass. A previous study found that the $PM_{2.5}/PM_{10}$ ratio ranged between 0.5–0.7 for six cities in China (Zhang *et al.*, 2004; Liu *et al.*, 2009a).

In this study, we analyzed the heavy haze episodes in January and February 2013 in Beijing, China. Because the peak $PM_{2.5}$ concentrations in Beijing reached 420 μg m^{-3}, which is 16 times the WHO standard for acceptable daily exposure (Alcorn, 2013), this event has been reported in several studies. For example, a study using data from 11 ground stations in central and eastern China pointed out that a major cause was the rapid secondary production of $PM_{2.5}$ due to abnormally high nitric oxide from fossil fuel combustion (Wang *et al.*, 2014). Another simulation study suggested that these severe $PM_{2.5}$ episodes were driven by stable synoptic weather conditions rather than abrupt increase in anthropogenic emissions. Another modelling study over Hebei province found that external contributions of $PM_{2.5}$ in three heavily polluted cities may have originated from different areas, emphasizing the importance to establish a regional emission control framework (Wang *et al.*, 2013a). However, none of these studies were designed to accurately estimate $PM_{2.5}$ concentration during this event. Using satellite data, ground observations and other publically available information, we developed daily $PM_{2.5}$ concentration contours using satellite remote sensing data and ground observations, respectively, and evaluated their utility of visualizing the spatial and temporal distributions of $PM_{2.5}$ levels in the North China plain centered in Beijing. We then investigated the factors that contributed to these severe particle pollution events. Furthermore, the method developed from this study will allow us to interpolate daily $PM_{2.5}$ concentrations and apply the data in the future research, including epidemiological study of the health impacts of air pollution, within the regions lacking ground monitoring stations.

DATA AND METHODS

Ground $PM_{2.5}$ Measurements

In February 2012, $PM_{2.5}$ was included in the Chinese National Ambient Air Quality Standard (CNAAQS, GB3095-2012, http://www.zzemc.cn/em_aw/Content/GB3095-2012.pdf). Since then, 24-hr $PM_{2.5}$ concentrations from all major Chinese cities have been published daily by the China National Environmental Monitoring Center (CNEMC) under the Chinese Ministry of Environmental Protection (MEP) (http://www.cnemc.cn/). Fig. 1 shows the topography and the spatial distribution of 258 ground monitors in our study area (latitude range: [36°N, 43°N], longitude range: [112°E, 121°E]). The low-elevation, heavily populated Beijing-Tianjin metropolitan area, Hebei Province, and Shandong Province are surrounded by the low hills in Liaoning Province to the northeast (~500–1,000m above sea level), by the Mongolian Plateau to the north and northwest (~1,500 m above sea level), by the Tai-hang Mountains in Shanxi province to the west (~1,000–1,500 m above sea level), and by the Bohai sea and Huanghai sea to the east. This highly industrialized area contains 19 large municipalities and part of another 44 municipalities. Air pollution dispersion is difficult at stagnation, or when southerly wind carries polluted air masses into Beijing. Fig. 1 also clearly shows the spatial clustering of monitoring stations in major cities whereas rural areas have little coverage. All the monitors are concentrated in ~30 large cities in our study region. For example, there are 35 monitors in and around the Beijing-Tianjin metropolitan area while the nearest monitoring station between Beijing and the neighboring Hebei Province, with several major coal-fired power plants south of Beijing, is at least 100 km away. This spatially biased sitting strategy ensures that the heavily polluted urban centers receive extensive coverage, but hinders the ability of the ground

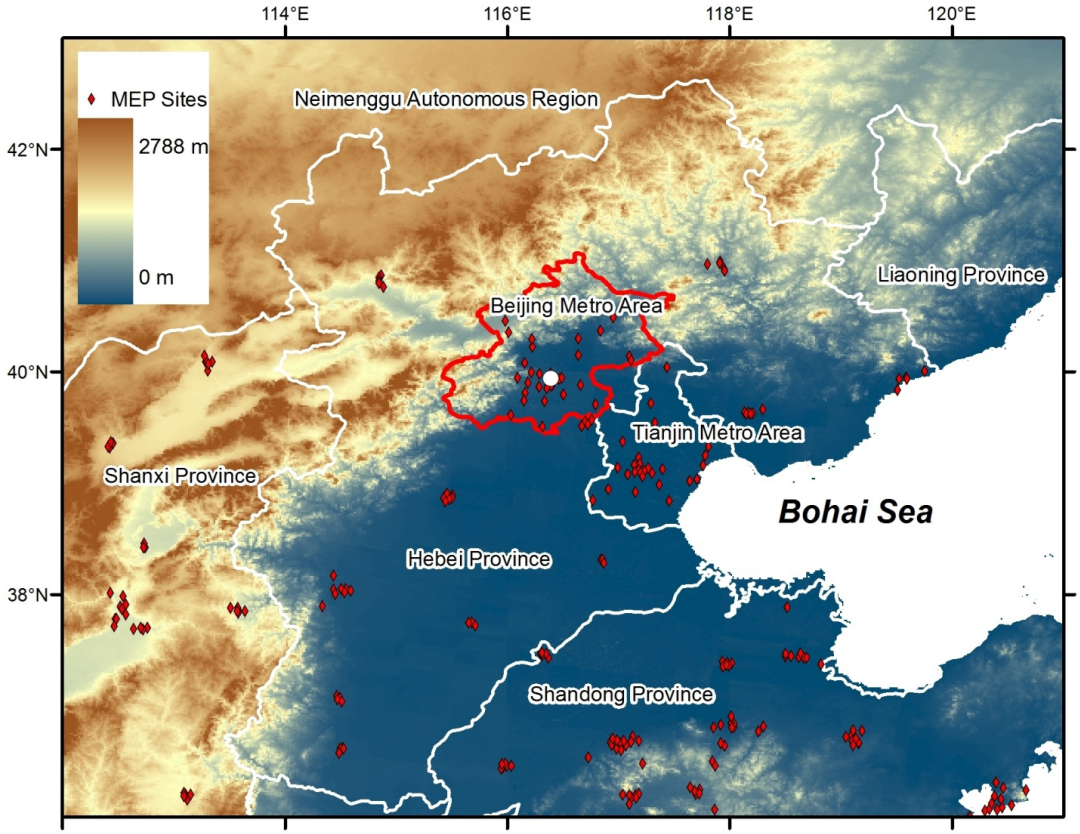

Fig. 1. Political borders (white for provincial borders, red for Beijing Metro Area), spatial distribution of MEP $PM_{2.5}$ monitoring stations (red diamonds) in the study area in North China, and the weather station in Beijing (white dot).

monitoring network to assess the impact of long-range pollution transport to local air quality.

Satellite Datasets: MODIS Collection 6 AOD Retrievals

For the current study, we used Collection 6 AOD products at a spatial resolution of 10 km retrieved by the Moderate Resolution Imaging Spectroradiometer (MODIS). The MODIS instruments, aboard both the Earth Observing System (EOS) Terra and Aqua satellites, cross the equator on the day side at approximately 10:30 a.m. and 1:30 p.m. local time, respectively (Remer *et al.*, 2005). Global validation studies showed that both Terra and Aqua MODIS AOD retrievals over land are highly correlated with ground observations from the AErosol RObotic NETwork (AERONET) (correlation coefficients ~0.9), and show little bias (Remer *et al.*, 2008; Levy *et al.*, 2010). Beijing's severe air pollution results in very high AOD especially during our study period. Standard MODIS Dark Target (DT) AOD cannot be retrieved over bright surfaces such as urban area with low coverage of vegetation. The Deep Blue (DB) algorithm was developed for retrieving AOD over bright-reflecting surfaces (Hsu *et al.*, 2013). However, previous version of DB AOD product has rarely been used in $PM_{2.5}$ studies due to its large retrieval errors. . In early 2014, the Aqua MODIS C6 AOD products retrieved by enhanced DT (Levy *et al.*, 2013) and Deep Blue (DB) algorithms (Hsu *et al.*, 2013) was released. We have developed a custom algorithm to combined DT and DB AOD products to optimize the AOD coverage (Ma *et al.*, 2015). Our results show that our combined AOD has a 50–100% coverage improvement in North China. A brief discussion of our AOD data fusion approached is provided in the Supplementary Materials (Text S2). For demonstration purpose, we used our combined AOD at 10 km resolution to estimate $PM_{2.5}$ concentration contours on January 17 and 18, 2013. All the MODIS data were downloaded from the NASA Goddard Space Flight Center MODIS Level 1 and Atmosphere Archive and Distribution System (http://ladsweb.nascom.nasa.gov).

Meteorological Data and HYSPLIT Trajectories

Although satellite AOD data can provide valuable information about the intensity and spatial impact of the haze event, they offer only limited information about aerosol movement (Pace *et al.*, 2005). In the current analysis, air parcel trajectories and meteorological parameters were combined with satellite measurements to analyze the influence of regional pollution transport on the air quality in Beijing. The HYSPLIT (HYbrid Single-Particle Lagrangian Integrated Trajectory) Model was developed by the National Oceanic and Atmospheric Administration (NOAA)'s Air Resources Laboratory and has been used extensively in air pollution transport studies (Draxier and Hess, 1998; Koukouli *et al.*, 2006). Developed by the National Centers for Environmental Prediction (NCEP), the Global Data Assimilation System (GDAS) model output at 0.5° × 0.5°

spatial resolution every three hours was used as the meteorological input for HYSPLIT simulations. Atmospheric boundary layer height (HPBL) data over Beijing were also extracted from raw GDAS data files to evaluate the impact of air pollution dispersion mixing on the formation of these episodes. The 48-hr backward air-parcel trajectories multiple receptor locations in Beijing were initialized at 500 m to 3 km above ground level to analyze the origin of the polluted air masses influencing the air quality of Beijing. Because the spatial resolution of GDAS meteorological fields are too coarse to resolve the impact of local land use types (i.e., highly developed urban center), the initiation height of the trajectories was set above the local surface roughness in order to correctly estimate general air mass movement. The maximum HPBL heights on January 13 (490 m) and 14 (730 m) were reached in early afternoon according to GDAS results. Therefore, the polluted air mass from south of Beijing could potentially be mixed with near surface air and affect ground $PM_{2.5}$ concentrations. In addition, hourly ground-level meteorological data such as temperature, relative humidity, wind speed, and precipitation of Beijing City were downloaded from a Weather Underground (Station ZBAA) in Beijing (39.939°N, 116.392°E) (http://www.wunderground.com/).

Data Processing and Analytical Approach

Daily city average $PM_{2.5}$ levels were calculated from all monitors within the Beijing Metropolitan area and used to analyze the temporal trend of $PM_{2.5}$ levels. The correlation between raw satellite AOD and ground $PM_{2.5}$ concentrations is often weak because $PM_{2.5}$-AOD relationship is strongly influenced by meteorological valuables such as relative humidity (Wang *et al.*, 2013b) and land use information (Liu *et al.*, 2009b). We developed a two-stage spatial statistical model to estimate ground $PM_{2.5}$ between January 1st and 28th using our combined AOD, meteorology variables including wind speed, precipitation, surface air pressure and planetary boundary layer height from Goddard Earth Observing System Data Assimilation System (GEOS 5-FP) (Lucchesi, 2013), land use data from European Space Agency (ESA) Global Land Cover Product (Bontemps *et al.*, 2011), and ground $PM_{2.5}$ concentrations. We used the first-stage linear mixed effect (LME) model to represent the temporal variations and the second-stage generalized additive model (GAM) with the smooth functions of geo-coordinates and land use parameters to represent the spatial heterogeneous. A detailed description of model structure is provided in the Supplementary Material (Text S1). Similar models have been successfully developed and applied in the Southeastern US (Hu *et al.*, 2014). Fig. 2 shows that the correlation between the estimated $PM_{2.5}$ based on the two-stage model and ground $PM_{2.5}$ concentrations is significantly improved ($R^2 = 0.73$; simple linear $PM_{2.5}$-combined AOD regression: $R^2 = 0.32$). Cross-validations results indicated that the selected interpolation method performs well on those $PM_{2.5}$ data (Supplementary Material, Fig. S1). We assessed the feasibility of using satellite remote sensing data to spatially examine the smog episodes in the entire study area. Next, for each selected days, we applied this model to derive the $PM_{2.5}$ concentrations (AOD-derived $PM_{2.5}$) wherever there are valid AOD retrievals within the study area. Daily contour maps of $PM_{2.5}$ concentrations estimated by our two-stage AOD model were generated using ordinary kriging techniques in ArcGIS 9.3 (Redlands, CA).

RESULTS AND DISCUSSION

Haze Episodes

A 60-day time-series of daily $PM_{2.5}$ (between December 24th, 2012 and February 21th, 2013) in Beijing (average of 35 monitoring stations) is shown in Fig. 3, upper panel. During this period, 38 days (63%) had $PM_{2.5}$ concentrations above the newly established CNAAQS daily $PM_{2.5}$ standard (75 μg m^{-3}), and 20 days (33%) had $PM_{2.5}$ twice above the standard (> 150 μg m^{-3}). The highest $PM_{2.5}$ concentration occurred on January 12th, 2013 (daily $PM_{2.5}$ = 427 μg m^{-3}).

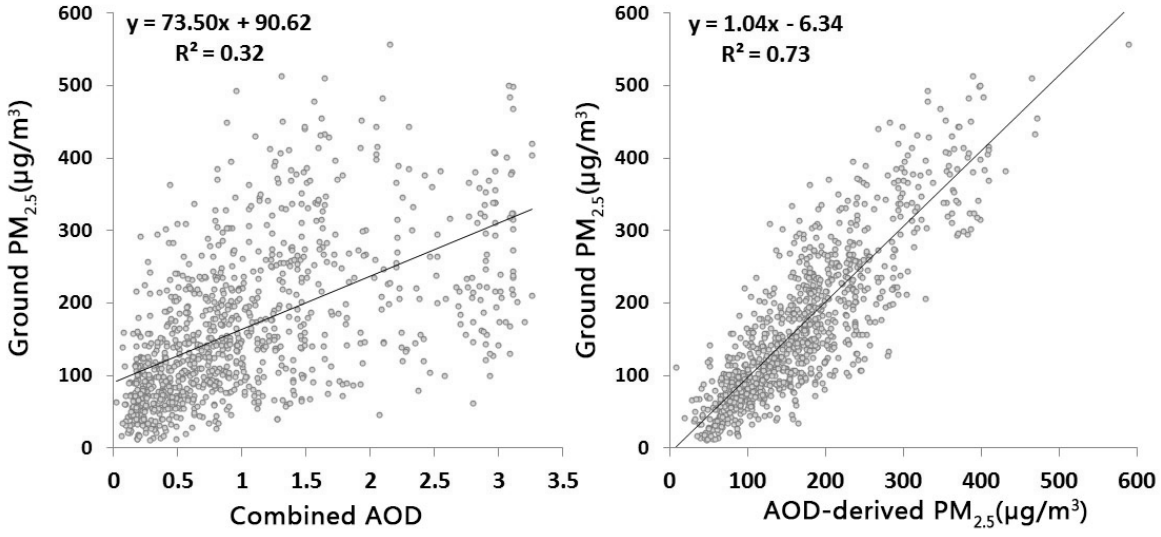

Fig. 2. Linear regression between raw combined AOD (left) or AOD-derived $PM_{2.5}$ (right) and ground $PM_{2.5}$ concentrations in North China (N = 995).

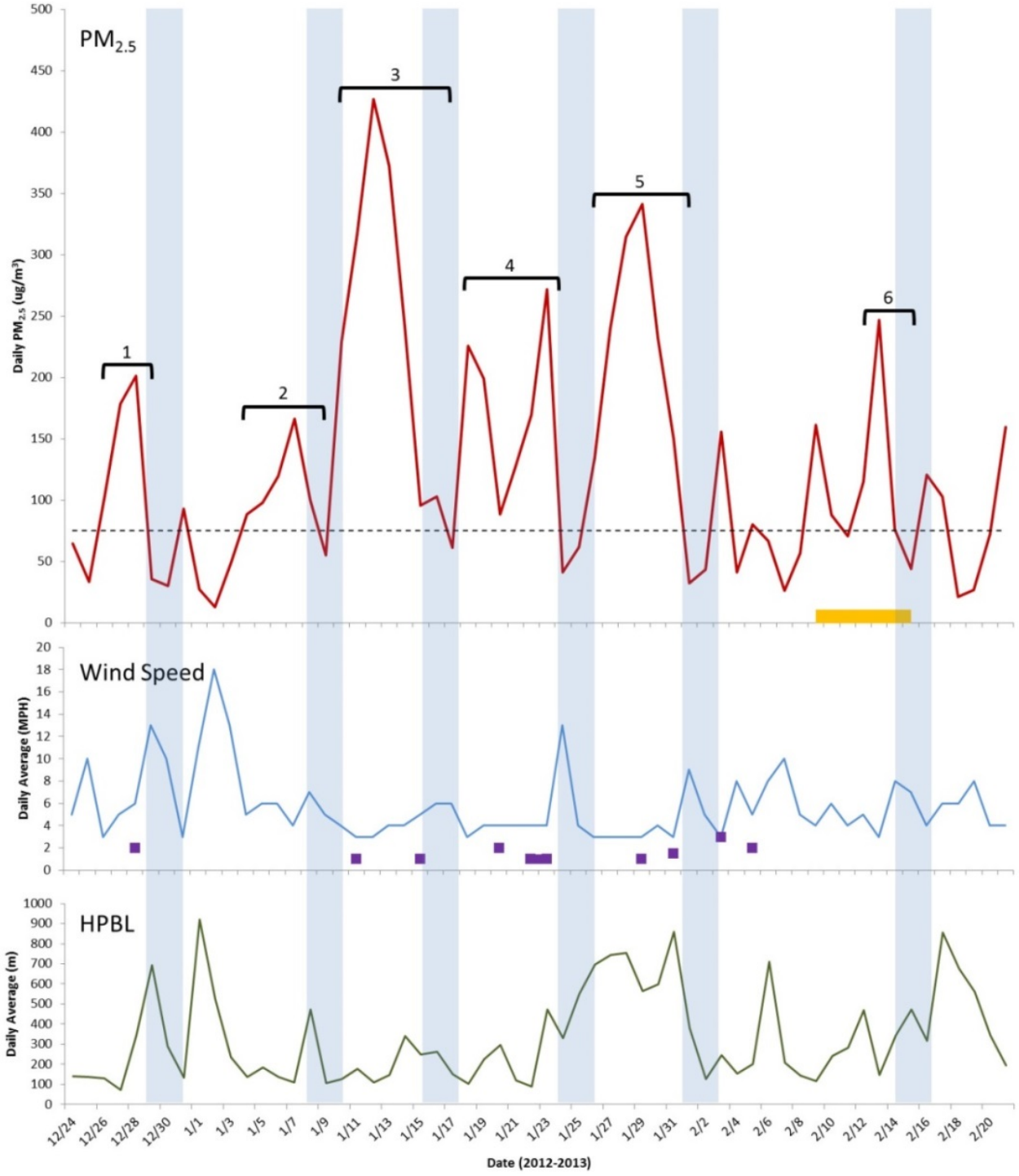

Fig. 3. Time series of daily variations of $PM_{2.5}$ and meteorological conditions between Dec 24th 2012 and Feb 21st 2012. *Upper Panel:* average $PM_{2.5}$ of entire geographic region of Beijing. Dash line indicates national standard for $PM_{2.5}$.The air pollution episodes were labeled by numbers. The orange color bar indicates a 7-day national holiday of Chinese New Year. *Middle Panel:* average daily wind speeds. (middle panel) and boundary layer height (HPBL) (lower panel). The purple dot/line in the middle panel indicates snow day(s) with at least 1 hour precipitation. *Lower Panel:* daily average HPBL. The light blue shade across all panels marks the wind clearing $PM_{2.5}$ between air pollution episodes.

Since there is no commonly accepted definition of a severe haze episode, we defined it as a period with ≥ 3 consecutive days of $PM_{2.5}$ above 75 μg m^{-3} (CNAAQS daily $PM_{2.5}$ standard) and at least one day having $PM_{2.5}$ > 150 μg m^{-3}. We identified six haze episodes within the 60-day observational window (Table 1). Two major episodes, characterized by high-level daily $PM_{2.5}$ (max daily concentration > 300 μg m^{-3}) and long duration (≥ 6 days), occurred in the mid-

and late-January. The 3rd episode, January 10th–16th, had an average daily $PM_{2.5}$ of 255 μg m^{-3}; and the 5th episode, January 26th–31st, average daily $PM_{2.5}$ = 235 μg m^{-3}). The last episode between February 12th and 14th, with a previous single-day increase of $PM_{2.5}$ on February 9th, occurred during the Chinese New Year (national holiday between February 9th and 15th). Celebration fireworks might have significantly contributed to the high $PM_{2.5}$ level.

Impacts of Weather Conditions

The identified smog episodes in Beijing were consistently associated with lower wind, and most episodes ended with strong or moderate winds (Fig. 3, middle panel). Pearson correlation coefficients also showed that $PM_{2.5}$ concentration was negatively correlated with the average wind speed of previous day ($r = –0.61$, $p < 0.001$). Although there were 10 snow days during this 60-day window, all snow events/days were light, without significant precipitation; therefore, this had little or no impact on clearing the air pollution. Low atmospheric boundary layer heights (HPBL) might also have affected $PM_{2.5}$ levels as we observed that the majority of air pollution episodes had low HPBLs on average (the first four episodes: 108 m, 204 m, 197 m, and 204 m, respectively), comparable with the average HPBL of the entire 60-day period (331 m) (Table 1). Of two major episodes (the 3rd and 5th), the latter had significantly higher HPBLs of 700 m, suggesting that it had a higher total loading of $PM_{2.5}$ than the 3rd episode. The last episode occurred during the Chinese New Year had a mean HPBL of 297 m. It should be noted that Fig. 3 (lower panel) showed that the HPBL can be as low as 100 m on some days. It is likely that the cold land surface generated a very stable boundary layer with little vertical mixing. As a result, HPBL is close to depth of the shallow radiation inversion layer. We also observed that $PM_{2.5}$ level was positively correlated with relative humidity ($r = 0.74$, $p < 0.001$), but not correlated with daily average temperature ($r = 0.21$, $p = 0.28$).

November 2012 through February 2013 was the coldest winter season in Beijing for the past 17 years. Starting on November 1st, the temperature of most days in November and December 2012 were consistently below the mean daily temperatures between 1996 and 2012 (Fig. 4, upper panel). December 2012 had the largest deviations of daily temperatures below average, and was the coldest month of the past 17 years (monthly mean temperature was 3.7°C below the 17-yearaverage). In addition to the cold weather, HPBL dropped significantly as a result of the temperature inversions caused by warm air coming from south of Beijing encountering the very cold Earth surface as well as night-time radiative cooling (Fig. 4, lower panel). The winter season led to a significant increase in energy consumption. Fig. 4 (middle panel) shows daily electricity generation and usage in the Beijing-Tianjin-Tangshan region (www.nengyuan.com, accessed on April 22). Compared with September and October, December 2012 had 22% and 16% increases in daily electricity usage and generation, respectively. The fluctuations of electricity usage and generation were smaller compared with $PM_{2.5}$ level changes as they were summaries of industrial and domestic use in suburban and rural areas of the entire region. This is consistent with a study of the synoptic weather patterns where it was found that meteorological conditions can explain up to 68% of the variability in visibility in eastern China (Zhang *et al.*, 2014). We observed similar increases of electricity usage and generation in adjacent provinces, including the southern parts of Hebei, Shandong, and Henan (data not shown). The missing data of electricity usage and generation in early February 2013 were due to the national holidays of the Chinese Lunar New Year.

Impacts of Regional Pollution Transport

An extremely cold winter season affected a much larger geographic region beyond Beijing metropolitan area, and many mega power plants using coal are located within this region. Thus, regional transport of PM could contribute to the air pollution episodes that occurred in Beijing in the winter of 2012–2013. Indeed, several adjacent cities in several southern provinces, including Hebei, Shandong, and Henan, had worse air quality than Beijing (data not shown), and many of these cities/regions harbor mega power plants that use coal. Fig. 5 shows the interpolated concentration contours of $PM_{2.5}$ using available ground monitoring data from January 2nd to 19th, 2013 in the study area, including the 2nd, 3rd, and the earlier part of the 4th smog episodes. Severe $PM_{2.5}$ pollution affected a large region covering Beijing, Tianjin, Hebei Province, and part of Shandong Province. The concentration contours indicated that the highest $PM_{2.5}$ levels were not in megacities, such as Beijing and Tianjin, but from several heavily industrialized regions in southern Hebei Province, which have several major coal-fired power plants. Moreover, northward regional transportation was also highly correlated with a decreasing pollutant gradient from south to north of Beijing. The 2nd,

Table 1. Summary of identified smog episodes in Beijing during the study period.

Episode	Date	Duration (days)	Mean $PM_{2.5}$ Concentration (μg m^{-3})	Max Daily $PM_{2.5}$ concentration (μg m^{-3})	Mean HPBL (meters)
1	Dec 26–28, 2012	3	161	201	108
2	Jan 4–8, 2013	5	114	166	204
3	Jan 10–16, 2013	7	255	427	197
4	Jan 18–23, 2013	6	180	272	204
5	Jan 26–31, 2013	6	235	341	700
6	Feb 12–14, 2013	3	146	247	297

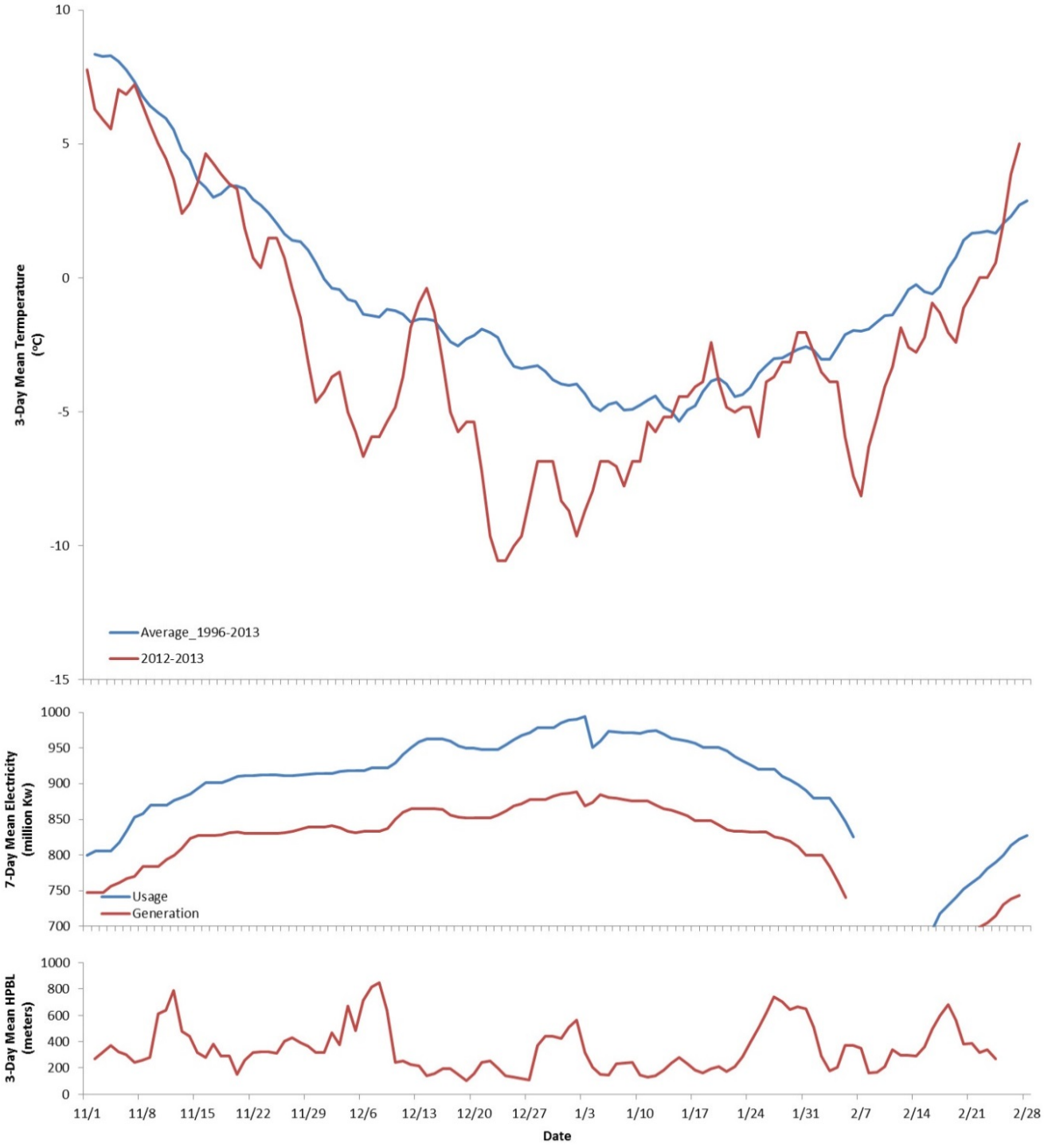

Fig. 4. Time series of daily temperature (upper panel) compared with daily electricity usage/generation (middle panel) and HPBL (lower panel) between Nov 1st 2012 and Feb 28st 2012.

3rd, and 4th smog episodes in Beijing were separated by cleaner days January 9th and January 17th. On both days, Beijing had moderate winds on the previous day from the northwest or north-northwest, which pushed the polluted air mass to the south of the city (gust speed of 36 km/hour, daily average wind speed 11 km hour^{-1} on January 8th and gust speed of 21 km hour^{-1}, daily average wind speed 10 km hour^{-1} on January 16th).

To examine qualitatively the impact of regional pollution transport, we constructed 48-hr backward air mass trajectories initiated at 8 am local time on January 13, 2013 from eight receptors evenly distributed in the Beijing Metro Area (Fig. 6). Originating at four altitudes above-ground, these trajectories show distinctly different patterns. At 500 m above-ground, all but one air mass trajectory on January 13 originated from the southern part of Hebei Province.

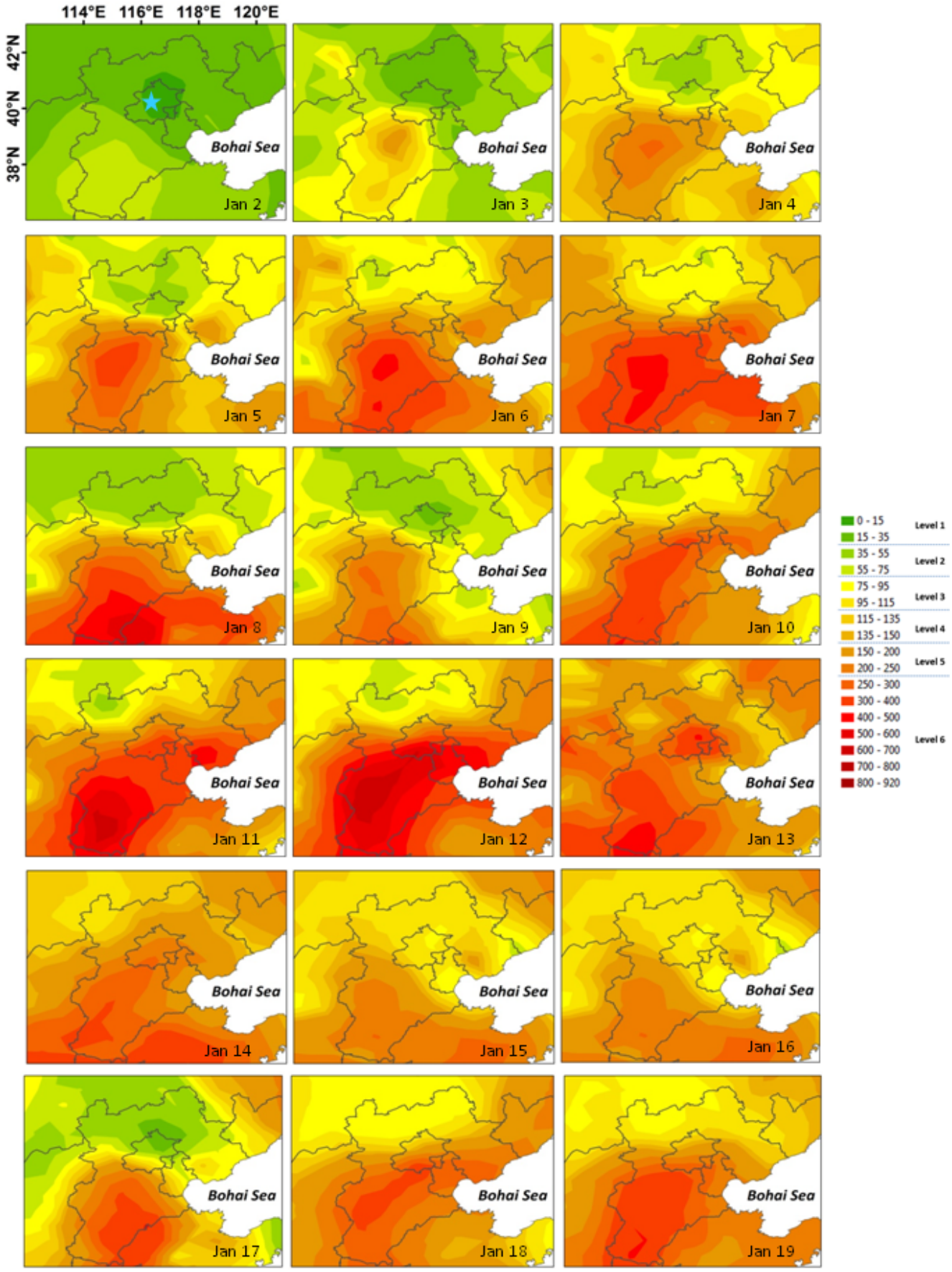

Fig. 5. Interpolated concentration contours in the Beijing-Tianjin-Hebei metropolitan area.

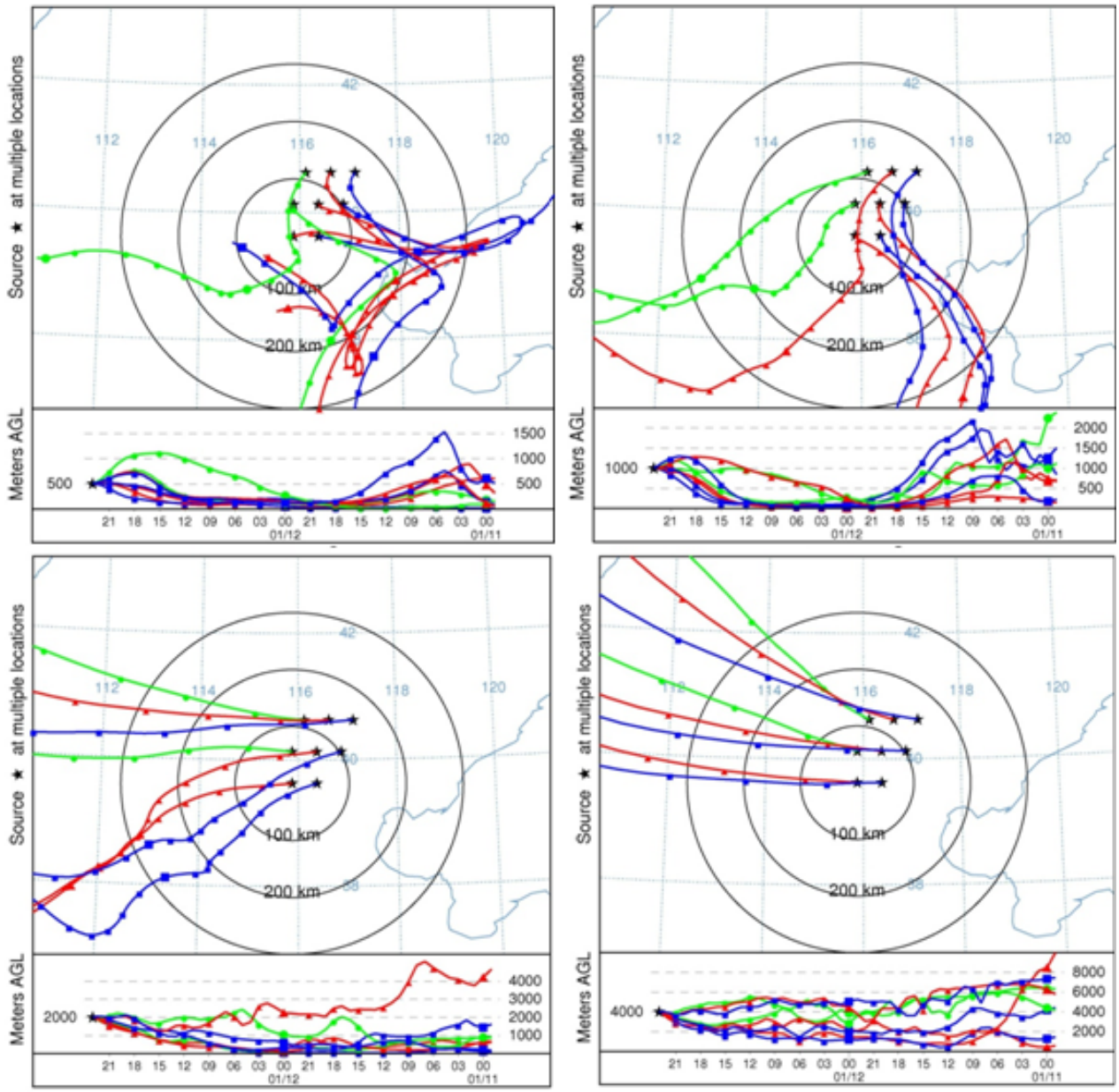

Fig. 6. HYSPLIT 48-hr backward trajectories initiated at 8 am local time on January 13th, 2013 from multiple receptors in Beijing at 500 m, 1000 m, 2000m and 4000m above the ground. Note: HYSPLIT time stamps are for UTC time. Beijing is in China Standard Time zone (UTC+8 hours).

During the transport process, the trajectories stayed close to the ground most of the time and temporarily moved over the Bo Hai Sea. At 1,000 m above-ground, the trajectories from the receptors in northwest Beijing originated from approximately 300 km southwest of Beijing. The other trajectories traveled over Shandong Province and the Tianjin metropolitan area. At 2,000 m level, which is above the average HPBL height during the 3rd episode in Beijing (Table 1), trajectories arrived from west Beijing over the Mongolian Plateau. Those from the receptors in the southern part of Beijing came from the southwest and traveled through much of Hebei Province. At 4000 m level, which is much higher than the winter boundary layer in Beijing, all the trajectories came from the Mongolian Plateau.

Satellite-Based Remote Sensing for Regional Transport

Fig. 7 compares $PM_{2.5}$ contour maps created with ground measurements and with satellite data on January 17th (daily $PM_{2.5}$ = 61 μg m^{-3}) and January 18th (daily $PM_{2.5}$ = 225 μg m^{-3}). Although $PM_{2.5}$ concentrations in Beijing were relatively low on January 17th, contours interpolated from both ground measurements and satellite remote sensing data clearly show a large polluted air mass with a $PM_{2.5}$ concentration above 140 μg m^{-3} south and southwest of Beijing. As this air mass moved northward on January 18th, it caused a sharp increase in $PM_{2.5}$ levels in Beijing. Although ground-based $PM_{2.5}$ contours corroborate the monitoring data at the site locations, these contours incorrectly assigned high pollution levels to these regions from monitoring

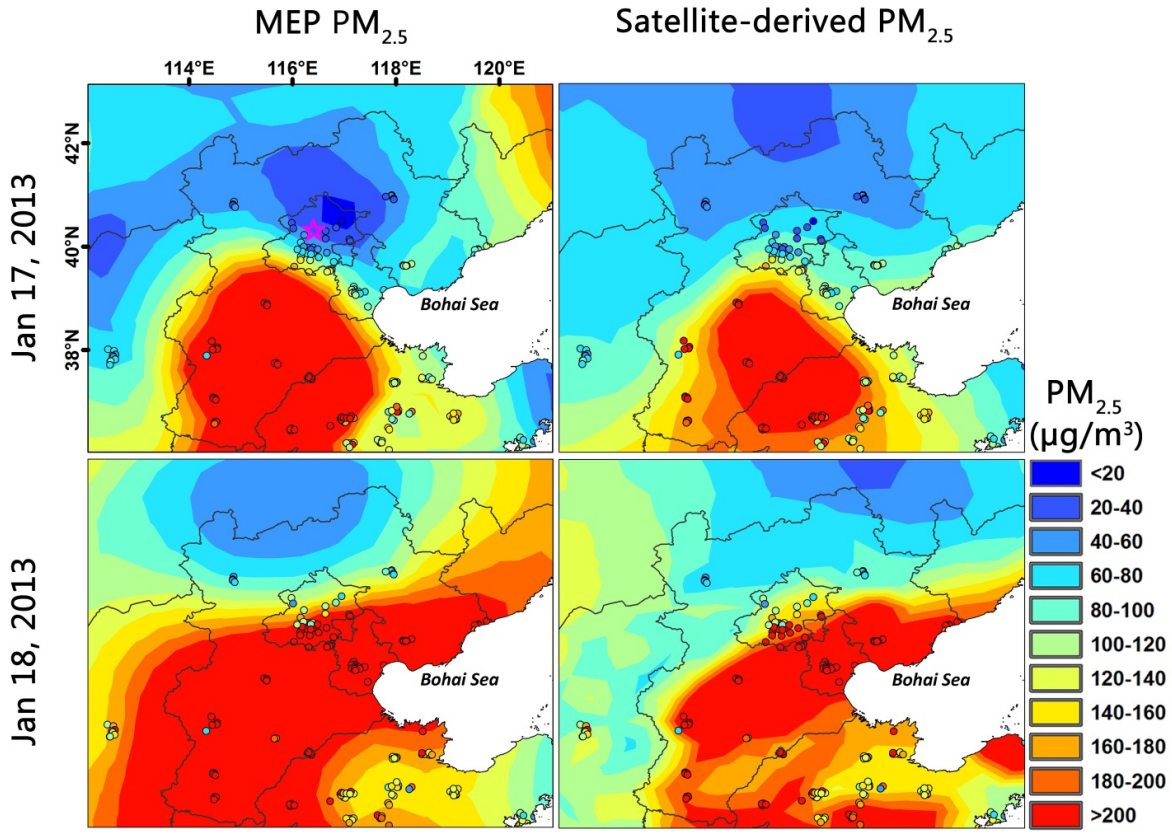

Fig. 7. Contours of $PM_{2.5}$ interpolated from ground measurements (left column) and MODIS-derived $PM_{2.5}$ estimates (right column) on January 17 and 18, 2013.

stations located in the highly polluted cities west of the mountain ranges. These satellite-based contours displayed a more meaningful terrain-following spatial structure of $PM_{2.5}$ concentrations because the contours were based on more comprehensive coverage of MODIS data at 10 km resolution.

DISCUSSION

We found that most of the highly polluted days during our 60-day observation window occurred in January, with 24 days of daily $PM_{2.5}$ above the national standard (75 μg m^{-3}). This standard is three times the WHO guideline for 24-hr average $PM_{2.5}$ (25 μg m^{-3}) (WHO, 2005) and more than twice the U.S. EPA 24-hr standard (35 μg m^{-3}). PM_{10} concentrations estimated from air quality indices released by the Beijing Municipal Environmental Protection Bureau suggests that January 2013 has the highest monthly pollution level for the past five winters (including November, December, and January of the past five years) (Supplementary Material, Fig. S2). We explored the potential mechanisms of the unusual extreme air pollution events. Extremely cold weather in December 2012 seems to have strong impacts on both the production and removal of $PM_{2.5}$. Cold weather increased energy consumption and, thus, air pollution emission. According to the China Information Industry Association (www.nengyuan.com), the regional electricity usage and generation were inversely related to daily mean temperature, and peaked around the coldest day of the season (Fig. 4, middle plot). Cold weather indirectly affected lower boundary layer height, which limited pollution dilution via convection. A long period of freezing temperatures chilled and kept the surface of earth very cold. As the temperature gradually increased after the coldest day, warm air from south Beijing moved over the cold earth surface and resulted in temperature inversions as seen in the generally low HPBL in the 60-day study period. Temperature inversions can significantly limit convection, therefore trapping fine particles near the surface. Thus, for the same loading of $PM_{2.5}$, a lower boundary layer can significantly increase the pollutant concentrations near the surface. Low HPBL could be an important meteorological factor leading to episodes 1 to 4 (Fig. 2). The severe air pollution in January, 2013 in Beijing shared some similarity with the famous London Smog event in December 1952 in which November 1952 was also an extremely cold month (Supplementary Material, Fig. S3). Moreover, a study of data collected from 11 ground monitoring sits of the Care-China Network (Campaign on the atmospheric Aerosol Research net-work of China) revealed that the unusual atmospheric circulation and the depression of strong cold air activities were the external causes of the severe smog episodes, and the quick secondary transformation of primary gaseous pollutants to secondary aerosols was the internal cause. Both internal and external causes contributed to the "explosive growth" and "sustained growth" of $PM_{2.5}$

(Wang *et al.*, 2014). In addition to extremely cold weather creating pre-depositing conditions, sustained abnormal climates, such as a weak East Asian winter monsoon, over eastern China in January 2013 also contributed to the development of smog episodes (Zhang *et al.*, 2014).

Weather conditions often affect a large geographic region. Cold weather has widespread impact on air pollution as pollutants are transported from highly polluted regions to adjacent, less polluted regions. Inspection of the daily $PM_{2.5}$ concentration contours allowed us to analyze the spatial scope of the severe smog events in the winter of 2013 in Beijing and its surrounding regions. In this study, we adopted the map concept of contour lines for pollutant concentrations to directly visualize and study the regional distribution of air pollutants. Moreover, daily change of contour lines within the same regional map can reveal spatial and temporal variations of air pollutants, which allow us to track the direction of transported pollutants and evaluate its impact. Our results revealed that the area affected by these smog events covered much of the North China Plain. The polluted area covered the two mega cities Beijing and Tianjin, as well as several provinces, such as Hebei, Henan, and Shandong, corresponding to a total area of ~570,000 km^2 and ~180 million people. These contour maps also indicated that although Beijing is the highest-profile city, it was not the most polluted one during these episodes. Ground measurements showed that the highest level of $PM_{2.5}$ was moving among heavily industrialized cities, south and southwest of Beijing, southern Hebei province and western Shandong province. It appears that, in winter, a significant portion of $PM_{2.5}$ in Beijing was contributed by long-range transport. Similar findings have been reported by previous simulation studies (Streets *et al.*, 2007). Besides our direct visualization, model simulations also supported regional transport as a significant resource of smog episodes. In this study, however, the ground monitor data collected from the same source of our study was only used for evaluating of the simulation results of Mesoscale Modeling System Generation 5 (MM5) and the Models-3/Community Multiscale Air Quality (CMAQ) modeling system applied in East Asia and the northern China with the Multi-resolution Emission Inventory of China (MEIC) (Wang *et al.*, 2013a).

Northwesterly and northerly winds from Siberia and the Mongolian Plateau were closely linked to the PM removal process. However, if the wind is transitory, not strong enough, or does not affect the entire polluted region, its clearing effect can be limited. For example, the moderate northwesterly wind (gust speed of 36 km $hour^{-1}$, daily average wind speed 11 km/hour) in Beijing on January 8th was only able to create a one-day narrow northwest to southeast corridor of low air pollution on January 9th, although most pollutants still existed along the corridor (Fig. 5). Once the wind stopped, the polluted condition was restored mostly by local emission. A similar scenario happened on January 17th when moderate wind speed barely pushed the polluted air mass in Beijing to its adjacent areas, resulting in a partially cleared corridor. Because northwesterly and northerly winds in winter in the North China Plain usually last only a few days (Wang *et al.*, 2009), severe air pollution is becoming common in this highly industrialized region. Without effective scavenging processes such as significant precipitation, severe smog episodes are likely to occur repeatedly due to high regional PM loading.

The accuracy of interpolated $PM_{2.5}$ concentration contours depends on the number and distribution of input data. In the case of the ground measurements, the current monitoring network is heavily biased towards urban centers with poor coverage outside large cities. For example, several monitoring stations are located in four large cities along the flat-bottomed land west of the Taihang Mountain, which runs down the eastern edge of the Loess Plateau (Fig. 1). The resulting $PM_{2.5}$ concentration contours represent urban air pollution levels well, but fail to differentiate the rural and high-elevation mountainous regions from the highly polluted urban low-land areas (Fig. 7). Compared with ground monitoring, the satellite-based contours were based on gridded AOD measurements with uniform coverage of the entire study area. Under cloud-free conditions, satellite-based contours tend to better represent the spatial heterogeneity of $PM_{2.5}$ by capturing the rural-urban contrast.

CONCLUSIONS

The severe Beijing smog of early 2013 was by multiple prolonged and severe smog events characterized by very high-level of $PM_{2.5}$ concentrations. Our analysis with ground observations indicated that temperature inversions resulted from a very cold winter, increased energy consumption in response to a higher heating demand, as well as long range transport of air pollution from south of Beijing are major contributors. The HYSPLIT trajectories indicated that polluted air masses from the southern parts of Hebei Province could reach Beijing in less than two days, therefore emission control measures need to be taken at regional level in order to be effective. To examine the impact of pollution transport on Beijing's air quality, current ground monitoring network may not be sufficient due to poor coverage in rural areas. Finally, satellite remote sensing data, if properly calibrated with meteorological parameters and ground observations, can provide realistic terrain-following spatial distribution of $PM_{2.5}$ concentrations to fill the gaps left by ground monitors.

ACKNOWLEDGMENTS

This work was supported by the National Natural Science Foundation of China (Grant No. 41471367), and the Foundation of Institute of Remote Sensing and Digital Earth, the Chinese Academy of Sciences (Y3SJ5900CX).

SUPPLEMENTARY MATERIALS

Supplementary data associated with this article can be found in the online version at http://www.aaqr.org.

REFERENCES

Alcorn, T. (2013). China's Skies: A Complex Recipe for Pollution with No Quick Fix. *Lancet* 381: 1973–1974.

Bell, M.L., Davis, D.L. and Fletcher, T. (2004). A Retrospective Assessment of Mortality from the London Smog Episode of 1952: The Role of Influenza and Pollution. *Environ. Health Perspect.* 112: 6–8.

Bontemps, S., Defourny, P., Bogaert, E.V., Arino, O., Kalogirou, V. and Perez, J.R. (2011). Globcover 2009-Products Description and Validation Report.

Chan, C.K. and Yao, X. (2008). Air Pollution in Mega Cities in China. *Atmos. Environ.* 42: 1–42.

Chen, T.M., Shofer, S., Gokhale, J. and Kuschner, W.G. (2007). Outdoor Air Pollution: Overview and Historical Perspective. *Am. J. Med. Sci.* 333: 230–234.

Draxier, R.R. and Hess, G.D. (1998). An Overview of the Hysplit_4 Modelling System for Trajectories, Dispersion and Deposition. *Aust. Meteorol. Mag.* 47: 295–308.

Hoff, R.M. and Christopher, S.A. (2009). Remote Sensing of Particulate Pollution from Space: Have We Reached the Promised Land? *J. Air Waste Manage. Assoc.* 59: 645–675.

Hsu, N., Jeong, M.J., Bettenhausen, C., Sayer, A., Hansell, R., Seftor, C., Huang, J. and Tsay, S.C. (2013). Enhanced Deep Blue Aerosol Retrieval Algorithm: The Second Generation. *J. Geophys. Res.* 118: 9296–9315.

Hu, X., Waller, L.A., Al-Hamdan, M.Z., Crosson, W.L., Estes Jr, M.G., Estes, S.M., Quattrochi, D.A., Sarnat, J.A. and Liu, Y. (2013). Estimating Ground-Level $PM_{2.5}$ Concentrations in the Southeastern U.S. Using Geographically Weighted Regression. *Environ. Res.* 121: 1–10.

Hu, X., Waller, L.A., Lyapustin, A., Wang, Y., Al-Hamdan, M.Z., Crosson, W.L., Estes, M.G., Estes, S.M., Quattrochi, D.A., Puttaswamy, S.J. and Liu, Y. (2014). Estimating Ground-Level $PM_{2.5}$ Concentrations in the Southeastern United States Using Maiac Aod Retrievals and a Two-Stage Model. *Remote Sens. Environ.* 140: 220–232.

Kloog, I., Nordio, F., Coull, B.A. and Schwartz, J. (2012). Incorporating Local Land Use Regression and Satellite Aerosol Optical Depth in a Hybrid Model of Spatiotemporal $PM_{2.5}$ Exposures in the Mid-Atlantic States. *Environ. Sci. Technol.* 46: 11913–11921.

Koukouli, M.E., Balis, D.S., Amiridis, V., Kazadzis, S., Bais, A., Nickovic, S. and Torres, O. (2006). Aerosol Variability over Thessaloniki Using Ground Based Remote Sensing Observations and the Toms Aerosol Index. *Atmos. Environ.* 40: 5367–5378.

Lee, H.J., Liu, Y., Coull, B.A., Schwartz, J. and Koutrakis, P. (2011). A Novel Calibration Approach of Modis Aod Data to Predict $PM_{2.5}$ Concentrations. *Atmos. Chem. Phys.* 11: 7991–8002.

Levy, R.C., Remer, L.A., Kleidman, R.G., Mattoo, S., Ichoku, C., Kahn, R. and Eck, T.F. (2010). Global Evaluation of the Collection 5 Modis Dark-Target Aerosol Products over Land. *Atmos. Chem. Phys.* 10: 10399–10420.

Levy, R., Mattoo, S., Munchak, L., Remer, L., Sayer, A., Patadia, F. and Hsu, N. (2013). The Collection 6 Modis Aerosol Products over Land and Ocean. *Atmos. Meas. Tech.* 6: 2989–3034.

Lim, S.S., Vos, T., Flaxman, A.D., Danaei, G., Shibuya, K., Adair-Rohani, H., Amann, M., Anderson, H.R., Andrews, K.G., Aryee, M., Atkinson, C., Bacchus, L.J., Bahalim, A.N., Balakrishnan, K., Balmes, J., Barker-Collo, S., Baxter, A., Bell, M.L., Blore, J.D., Blyth, F., Bonner, C., Borges, G., Bourne, R., Boussinesq, M., Brauer, M., Brooks, P., Bruce, N.G., Brunekreef, B., Bryan-Hancock, C., Bucello, C., Buchbinder, R., Bull, F., Burnett, R.T., Byers, T.E., Calabria, B., Carapetis, J., Carnahan, E., Chafe, Z., Charlson, F., Chen, H., Chen, J.S., Cheng, A.T.A., Child, J.C., Cohen, A., Colson, K.E., Cowie, B.C., Darby, S., Darling, S., Davis, A., Degenhardt, L., Dentener, F., Des Jarlais, D.C., Devries, K., Dherani, M., Ding, E.L., Dorsey, E.R., Driscoll, T., Edmond, K., Ali, S.E., Engell, R.E., Erwin, P.J., Fahimi, S., Falder, G., Farzadfar, F., Ferrari, A., Finucane, M.M., Flaxman, S., Fowkes, F.G.R., Freedman, G., Freeman, M.K., Gakidou, E., Ghosh, S., Giovannucci, E., Gmel, G., Graham, K., Grainger, R., Grant, B., Gunnell, D., Gutierrez, H.R., Hall, W., Hoek, H.W., Hogan, A., Hosgood, H.D., Hoy, D., Hu, H., Hubbell, B.J., Hutchings, S.J., Ibeanusi, S.E., Jacklyn, G.L., Jasrasaria, R., Jonas, J.B., Kan, H., Kanis, J.A., Kassebaum, N., Kawakami, N., Khang, Y.H., Khatibzadeh, S., Khoo, J.P., Kok, C., Laden, F., Lalloo, R., Lan, Q., Lathlean, T., Leasher, J.L., Leigh, J., Li, Y., Lin, J.K., Lipshultz, S.E., London, S., Lozano, R., Lu, Y., Mak, J., Malekzadeh, R., Mallinger, L., Marcenes, W., March, L., Marks, R., Martin, R., McGale, P., McGrath, J., Mehta, S., Mensah, G.A., Merriman, T.R., Micha, R., Michaud, C., Mishra, V., Hanafiah, K.M., Mokdad, A.A., Morawska, L., Mozaffarian, D., Murphy, T., Naghavi, M., Neal, B., Nelson, P.K., Nolla, J.M., Norman, R., Olives, C., Omer, S.B., Orchard, J., Osborne, R., Ostro, B., Page, A., Pandey, K.D., Parry, C.D.H., Passmore, E., Patra, J., Pearce, N., Pelizzari, P.M., Petzold, M., Phillips, M.R., Pope, D., Pope, C.A., Powles, J., Rao, M., Razavi, H., Rehfuess, E.A., Rehm, J.T., Ritz, B., Rivara, F.P., Roberts, T., Robinson, C., Rodriguez-Portales, J.A., Romieu, I., Room, R., Rosenfeld, L.C., Roy, A., Rushton, L., Salomon, J.A., Sampson, U., Sanchez-Riera, L., Sanman, E., Sapkota, A., Seedat, S., Shi, P., Shield, K., Shivakoti, R., Singh, G.M., Sleet, D.A., Smith, E., Smith, K.R., Stapelberg, N.J.C., Steenland, K., Stöckl, H., Stovner, L.J., Straif, K., Straney, L., Thurston, G.D., Tran, J.H., Van Dingenen, R., van Donkelaar, A., Veerman, J.L., Vijayakumar, L., Weintraub, R., Weissman, M.M., White, R.A., Whiteford, H., Wiersma, S.T., Wilkinson, J.D., Williams, H.C., Williams, W., Wilson, N., Woolf, A.D., Yip, P., Zielinski, J.M., Lopez, A.D., Murray, C.J.L. and Ezzati, M. (2012). A Comparative Risk Assessment of Burden of Disease and Injury Attributable to 67 Risk Factors and Risk Factor Clusters in 21 Regions, 1990?2010: A Systematic Analysis for the Global Burden of Disease Study 2010. *The Lancet* 380: 2224–2260.

Liu, Y., Sarnat, J.A., Kilaru, A., Jacob, D.J. and Koutrakis, P. (2005). Estimating Ground-Level $PM_{2.5}$ in the Eastern United States Using Satellite Remote Sensing. *Environ. Sci. Technol.* 39: 3269–3278.

Liu, Y., Chen, D., Kahn, R.A. and He, K.B. (2009a). Review of the Applications of Multiangle Imaging

Spectroradiometer to Air Quality Research. *Sci. China, Ser. D Earth Sci.* 52: 132–144.

Liu, Y., Paciorek, C.J. and Koutrakis, P. (2009b). Estimating Regional Spatial and Temporal Variability of $PM_{2.5}$ Concentrations Using Satellite Data, Meteorology, and Land Use Information. *Environ. Health Perspect.* 117: 886–892.

Loomis, D., Grosse, Y., Lauby-Secretan, B., Ghissassi, F.E., Bouvard, V., Benbrahim-Tallaa, L., Guha, N., Baan, R., Mattock, H. and Straif, K. (2013). The Carcinogenicity of Outdoor Air Pollution. *Lancet Oncol.* 14: 1262–1263.

Lucchesi, R. (2013). File Specification for Geos-5 Fp. Gmao Office Note No. 4 (Version 1.0). Available from Http://Gmao.Gsfc.Nasa.Gov/Pubs/Office_Notes.

Ma, Z.W., Hu, X.F., Huang, L., Bi, J. and Liu, Y. (2014). Estimating Ground-Level $PM_{2.5}$ in China Using Satellite Remote Sensing. *Environ. Sci. Technol.* 48: 7436–7444.

Ma, Z., Hu, X., Bi, J., Xue, Y., Huang, L. and Liu, Y. (2015). 10 Years of $PM_{2.5}$ Concentrations in China Estimated from Satellite Data and a Two-Stage Statistical Model. *Environ. Health Perspect.* Manuscript under Review.

Nemery, B., Hoet, P.H. and Nemmar, A. (2001). The Meuse Valley Fog of 1930: An Air Pollution Disaster. *Lancet* 357: 704–708.

Pace, G., Meloni, D. and di Sarra, A. (2005). Forest Fire Aerosol over the Mediterranean Basin During Summer 2003. *J. Geophys. Res.* 110: D21202, doi: 10.1029/2005 JD005986.

Pope, C.A. and Dockery, D.W. (2006). Health Effects of Fine Particulate Air Pollution: Lines That Connect. *J. Air Waste Manage. Assoc.* 56: 709–742.

Qu, W.J., Arimoto, R., Zhang, X.Y., Zhao, C.H., Wang, Y.Q., Sheng, L.F. and Fu, G. (2010). Spatial Distribution and Interannual Variation of Surface PM_{10} Concentrations over Eighty-Six Chinese Cities. *Atmos. Chem. Phys.* 10: 5641–5662.

Remer, L.A., Kaufman, Y.J., Tanre, D., Mattoo, S., Chu, D.A., Martins, J.V., Li, R.R., Ichoku, C., Levy, R.C., Kleidman, R.G., Eck, T.F., Vermote, E. and Holben, B.N. (2005). The Modis Aerosol Algorithm, Products, and Validation. *J. Atmos. Sci.* 62: 947–973.

Remer, L.A., Kleidman, R.G., Levy, R.C., Kaufman, Y.J., Tanre, D., Mattoo, S., Martins, J.V., Ichoku, C., Koren, I., Yu, H.B. and Holben, B.N. (2008). Global Aerosol Climatology from the Modis Satellite Sensors. *J. Geophy. Res.* 113: D14S07.

Song, C.K., Ho, C.H., Park, R.J., Choi, Y.S., Kim, J., Gong, D.Y. and Lee, Y.B. (2009). Spatial and Seasonal Variations of Surface PM_{10} Concentration and Modis Aerosol Optical Depth over China. *Asia-Pac. J. Atmos. Sci.* 45: 33–43.

Streets, D.G., Fu, J.H.S., Jang, C.J., Hao, J.M., He, K.B., Tang, X.Y., Zhang, Y.H., Wang, Z.F., Li, Z.P., Zhang, Q., Wang, L.T., Wang, B.Y. and Yu, C. (2007). Air Quality During the 2008 Beijing Olympic Games. *Atmos. Environ.* 41: 480–492.

Wang, L.T., Wei, Z., Yang, J., Zhang, Y., Zhang, F.F., Su, J., Meng, C.C. and Zhang, Q. (2013a). The 2013 Severe Haze over the Southern Hebei, China: Model Evaluation, Source Apportionment, and Policy Implications. *Atmos. Chem. Phys. Discuss.* 13: 28395–28451.

Wang, W., Primbs, T., Tao, S. and Simonich, S.L.M. (2009). Atmospheric Particulate Matter Pollution during the 2008 Beijing Olympics. *Environ. Sci. Technol.* 43: 5314–5320.

Wang, Y., Yao, L., Wang, L., Liu, Z., Ji, D., Tang, G., Zhang, J., Sun, Y., Hu, B. and Xin, J. (2014). Mechanism for the Formation of the January 2013 Heavy Haze Pollution Episode over Central and Eastern China. *Sci. China Earth Sci.* 57: 14–25.

Wang, Z.X., Liu, Y., Hu, M., Pan, X.C., Shi, J., Chen, F., He, K.B., Koutrakis, P. and Christiani, D.C. (2013b). Acute Health Impacts of Airborne Particles Estimated from Satellite Remote Sensing. *Environ. Int.* 51: 150–159.

WHO (World Health Organization) (2005). Who Air Quality Guidelines for Particulate Matter, Ozone, Nitrogen Dioxide and Sulfur Dioxide, Global Update 2005, Summary of Risk Assessment, World Health Organization, Geneva.

Yang, F., Tan, J., Zhao, Q., Du, Z., He, K., Ma, Y., Duan, F. and Chen, G. (2011). Characteristics of $PM_{2.5}$ Speciation in Representative Megacities and across China. *Atmos. Chem. Phys.* 11: 5207–5219.

Zhang, Q., He, K. and Huo, H. (2012). Policy: Cleaning China's Air. *Nature* 484: 161–162.

Zhang, R., Li, Q. and Zhang, R. (2014). Meteorological Conditions for the Persistent Severe Fog and Haze Event over Eastern China in January 2013. *Sci. China Earth Sci.* 57: 26–35.

Zhang, Y., Zhu, X., Slanina, S., Shao, M., Zeng, L., Hu, M., Bergin, M. and Salmon, L. (2004). Aerosol Pollution in Some Chinese Cities (Iupac Technical Report). *Pure Appl. Chem.* 76: 1227–1239.

Received for review, January 31, 2015
Revised, July 1, 2015
Accepted, August 26, 2015